CHAPTER 7

EXPERIMENTAL EVALUATION OF PROPOSED INDICES

Much of the work in the previous chapters has laid the foundation for the nonlinear index problem. The theory for the different evaluators of nonlinearity was explained, and a candidate for the extrapolation factor was selected. However, the theory behind the different indices is only approximate at best. Therefore, the only way to assess the different possible indices is experimentally. In this chapter, each of the proposed indicators are compared experimentally. The chapter begins by presenting the calculation of each of the indices for each of the data sets at the applied voltage settings. After that, the threshold values corresponding to the maximum acceptable amount of nonlinearity for each of the indicators for each data set is calculated and discussed. Finally, the performance for each of the indicators is evaluated, and some general observations are made on the choice of an indicator to limit voltage based linear extrapolation. The MATLAB code used to perform the analysis for this chapter is found in Appendix G.

7.1 Calculation of Indices at Each Applied Voltage

The method for calculating the indices from the measured waveform at the focus has already been discussed in Chapter 4. Therefore, in this section the calculated indices for each transducer and each drive will be presented. Since the goal was to find an indicator that would be applicable to any focused source under any drive condition, many different types of transducers and excitations were evaluated. In order to test insensitivity to frequency, transducers were selected with circuit resonant frequencies of approximately 3 MHz, 5.5 MHz and 8 MHz. Also, in order to confirm insensitivity to *f/#*, transducers with *f/#*'s of 1 and 2 were evaluated. Aperture size was also tested by selecting transducers with approximately the same frequency and *f/#* but having different

diameters. Furthermore, insensitivity to drive conditions was tested by driving one of the transducers with a “positive going” “three cycle” pulse, a “negative going” “three cycle” pulse, and a “positive going” “one cycle” pulse. A discussion of these terms is provided in Chapter 6. The results for all of these cases are presented in Figures 7.1-7.14.

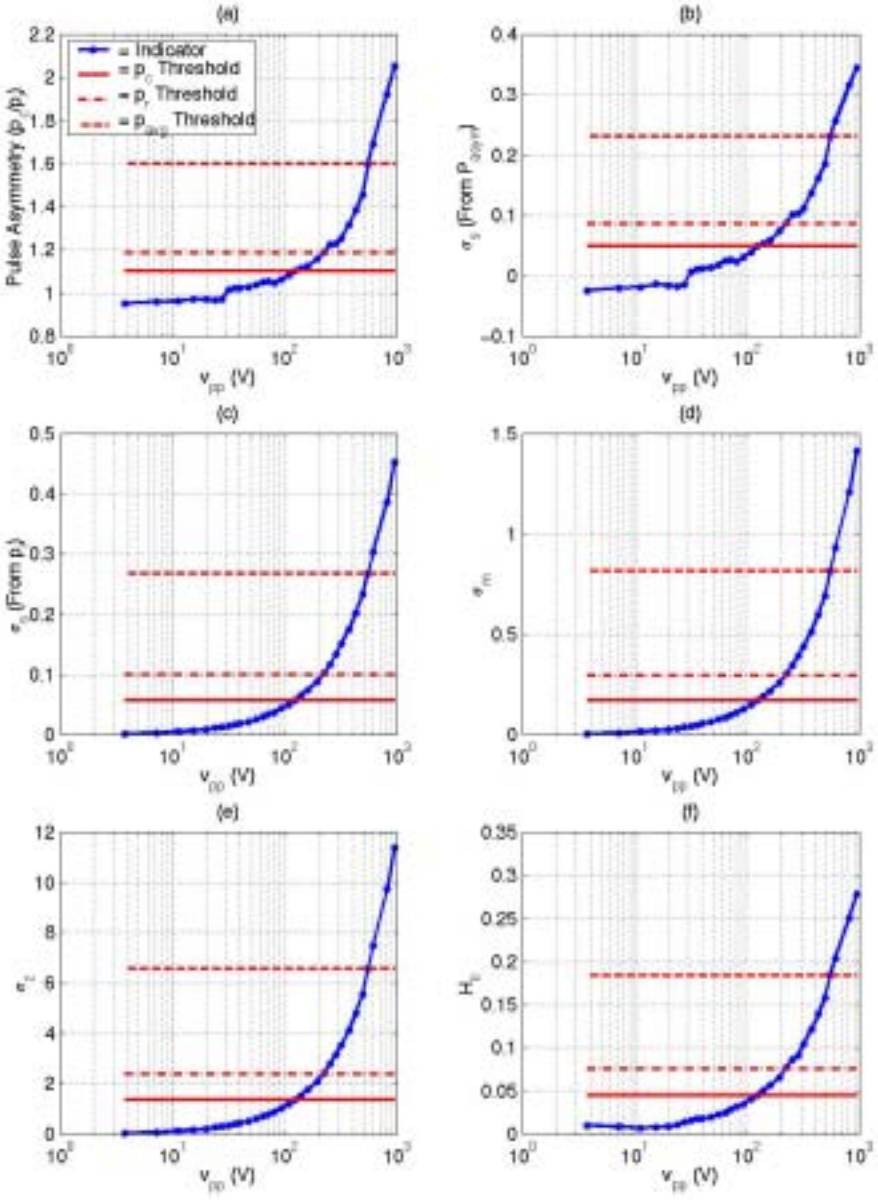

Figure 7.1 First six indicators for a 2.8072 MHz, *f/#* of 1, 1.905 cm diameter transducer excited by a “positive going” “three cycle” pulse. (a) Asymmetric ratio P_{asym}. (b) σ_s from P_{asym}. (c) σ_s from p_r. (d) σ_m. (e) σ_z. (f) Second harmonic ratio H_{II}.

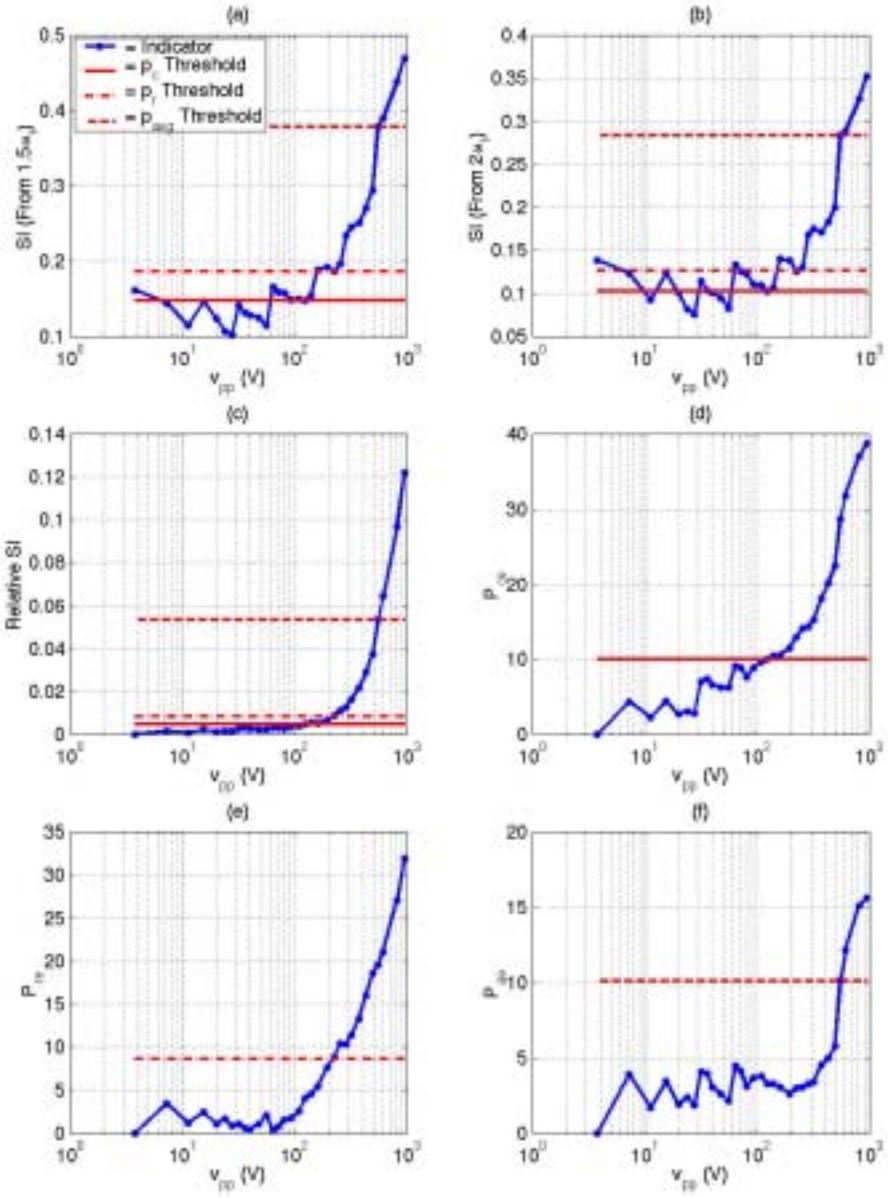

Figure 7.2 Second six indicators for a 2.8072 MHz, *f/#* of 1, 1.905 cm diameter transducer excited by a "positive going" "three cycle" pulse. (a) *si* from $1.5\omega_1$. (b) *si* from $2\omega_1$. (c) *rsi*. (d) P_{ce}. (e) P_{re}. (f) P_{ae}.

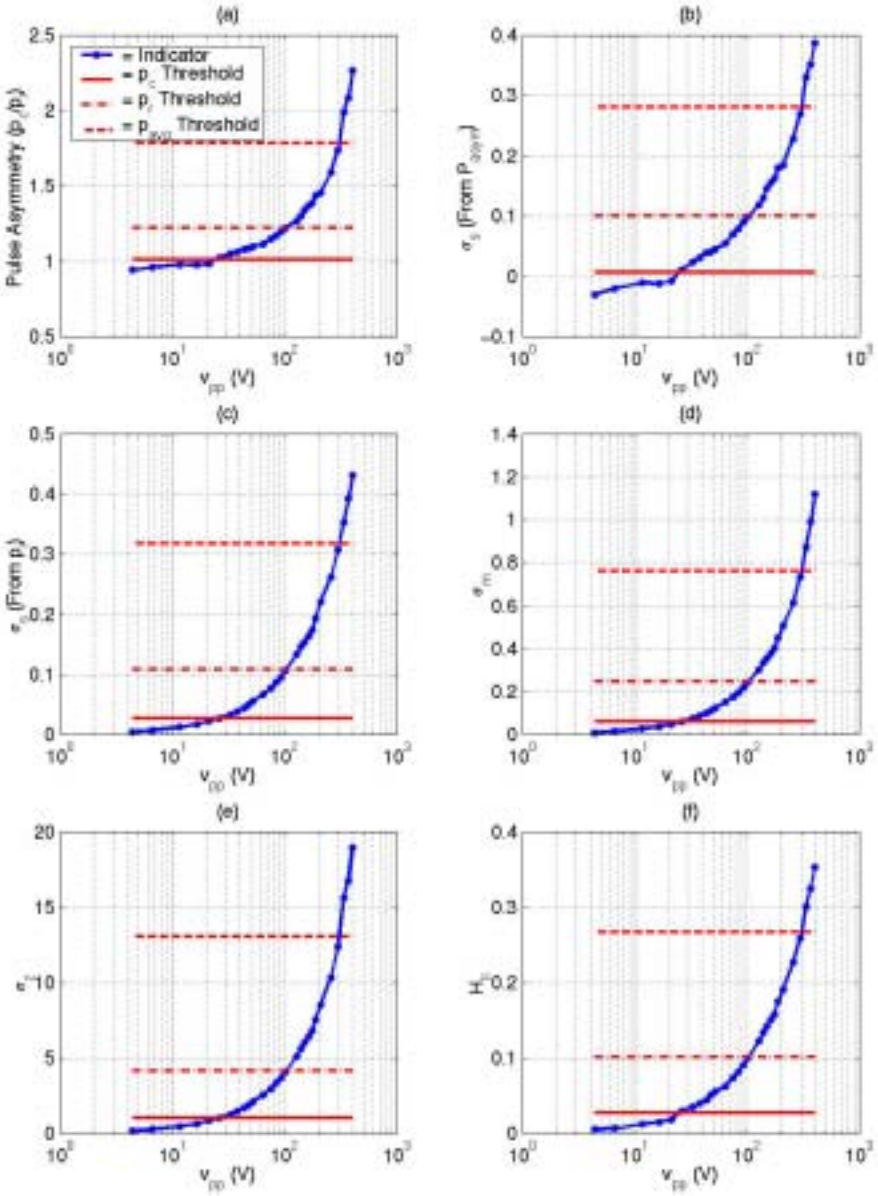

Figure 7.3: First six indicators for a 2.9983 MHz, *f/#* of 1, 5.08 cm diameter transducer excited by a "positive going" "three cycle" pulse. (a) Asymmetric ratio P_{asym}. (b) σ_s from P_{asym}. (c) σ_s from p_r. (d) σ_m. (e) σ_z. (f) Second harmonic ratio H_{II}.

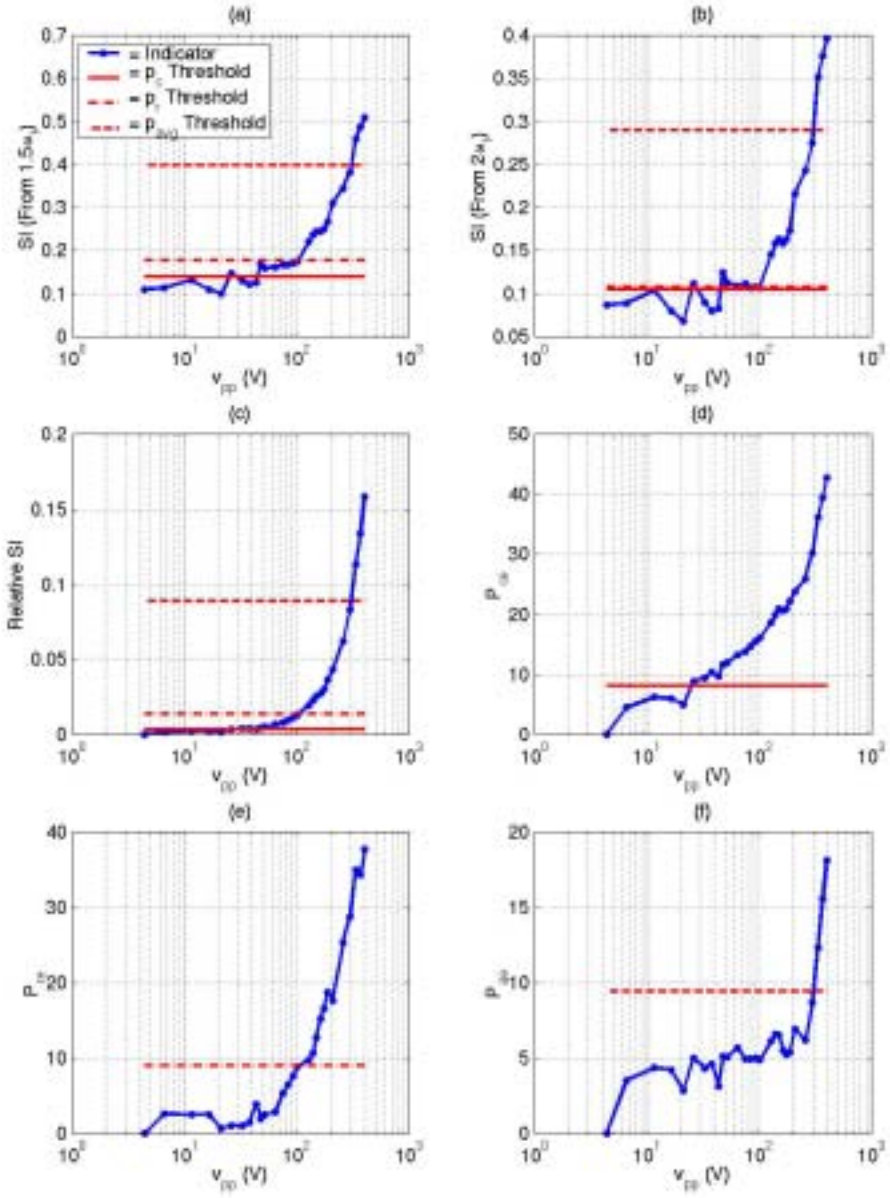

Figure 7.4 Second six indicators for a 2.9983 MHz, *f/#* of 1, 5.08 cm diameter transducer excited by a "positive going" "three cycle" pulse. (a) *si* from $1.5\omega_1$. (b) *si* from $2\omega_1$. (c) *rsi*. (d) P_{ce}. (e) P_{re}. (f) P_{ae}.

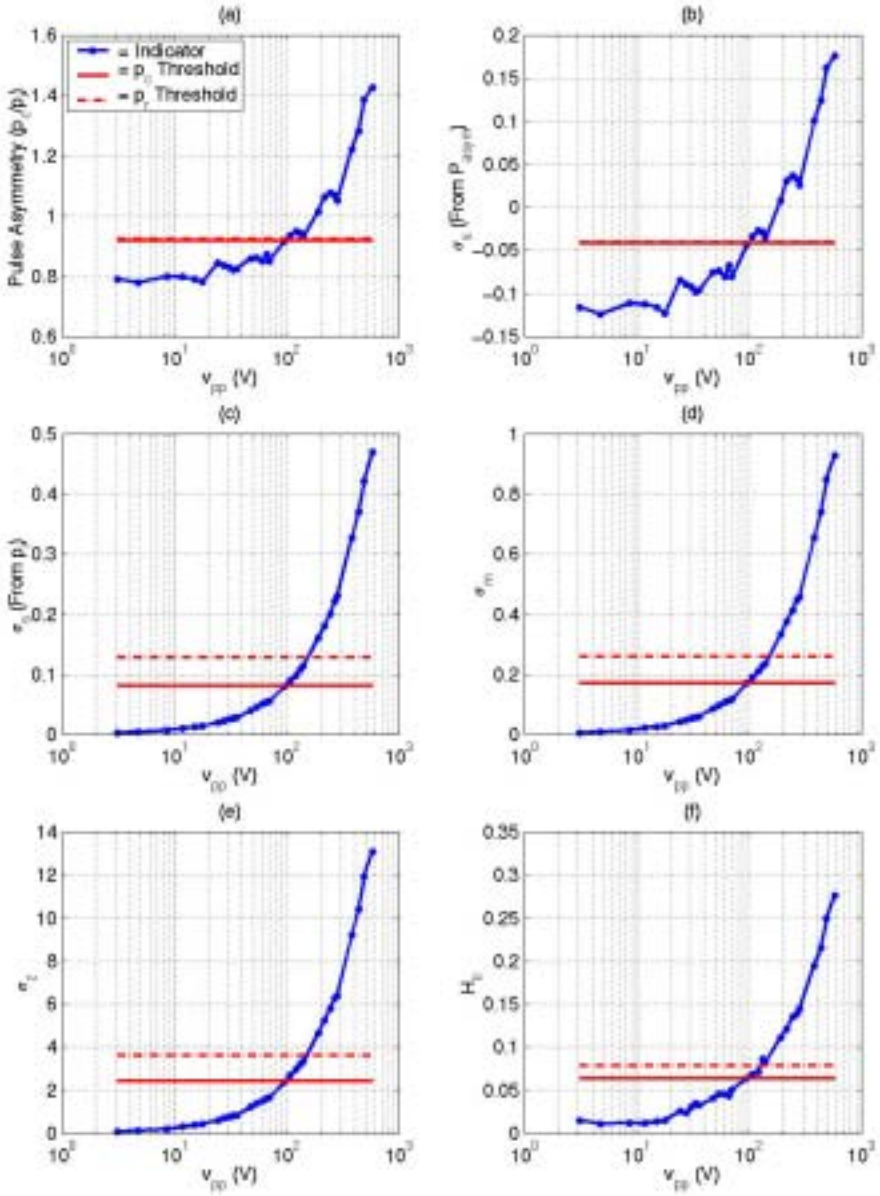

Figure 7.5: First six indicators for a 5.4906 MHz, *f/#* of 1, 1.905 cm diameter transducer excited by a "positive going" "one cycle" pulse. (a) Asymmetric ratio P_{asym}. (b) σ_s from P_{asym}. (c) σ_s from p_r. (d) σ_m. (e) σ_z. (f) Second harmonic ratio H_{II}.

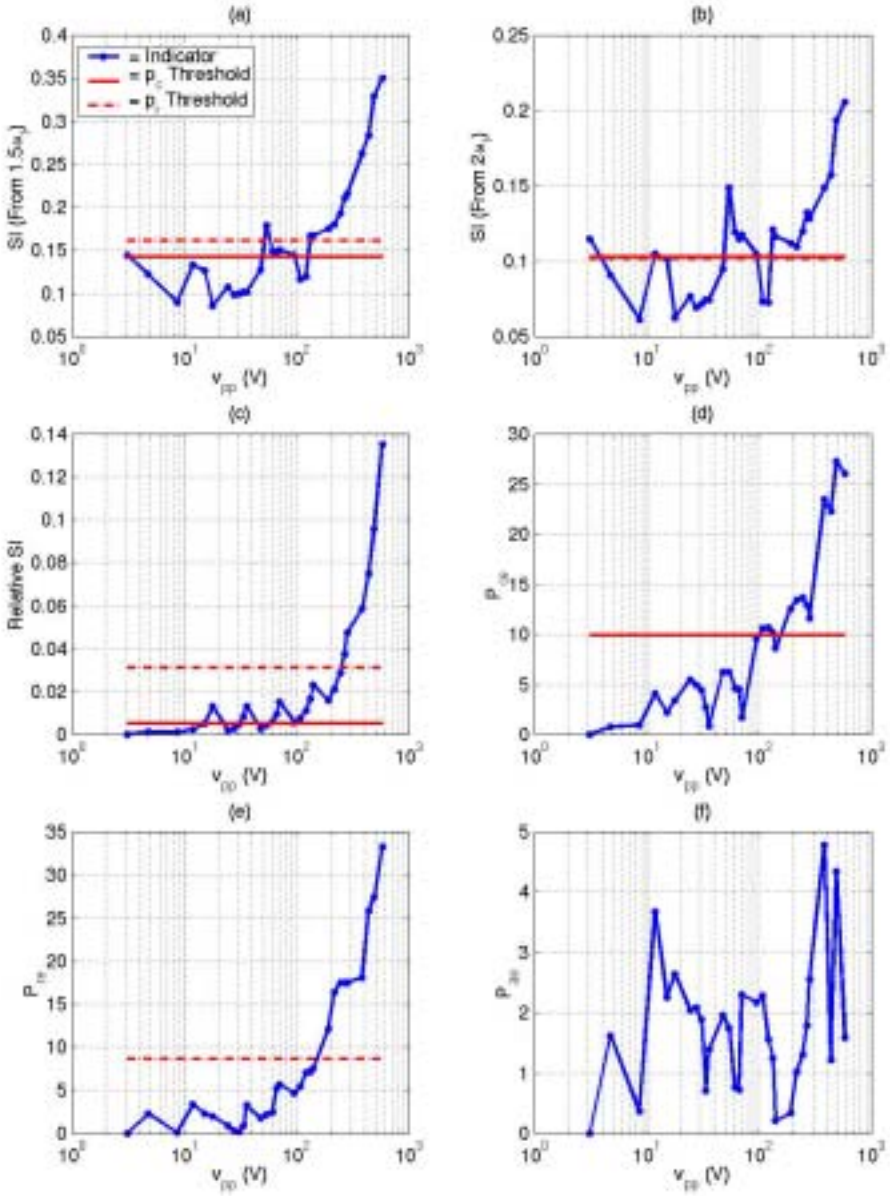

Figure7.6: Second six indicators for a 5.4906 MHz, *f/#* of 1, 1.905 cm diameter transducer excited by a "positive going" "one cycle" pulse. (a) *si* from $1.5\omega_1$. (b) *si* from $2\omega_1$. (c) *rsi*. (d) P_{ce}. (e) P_{re}. (f) P_{ae}.

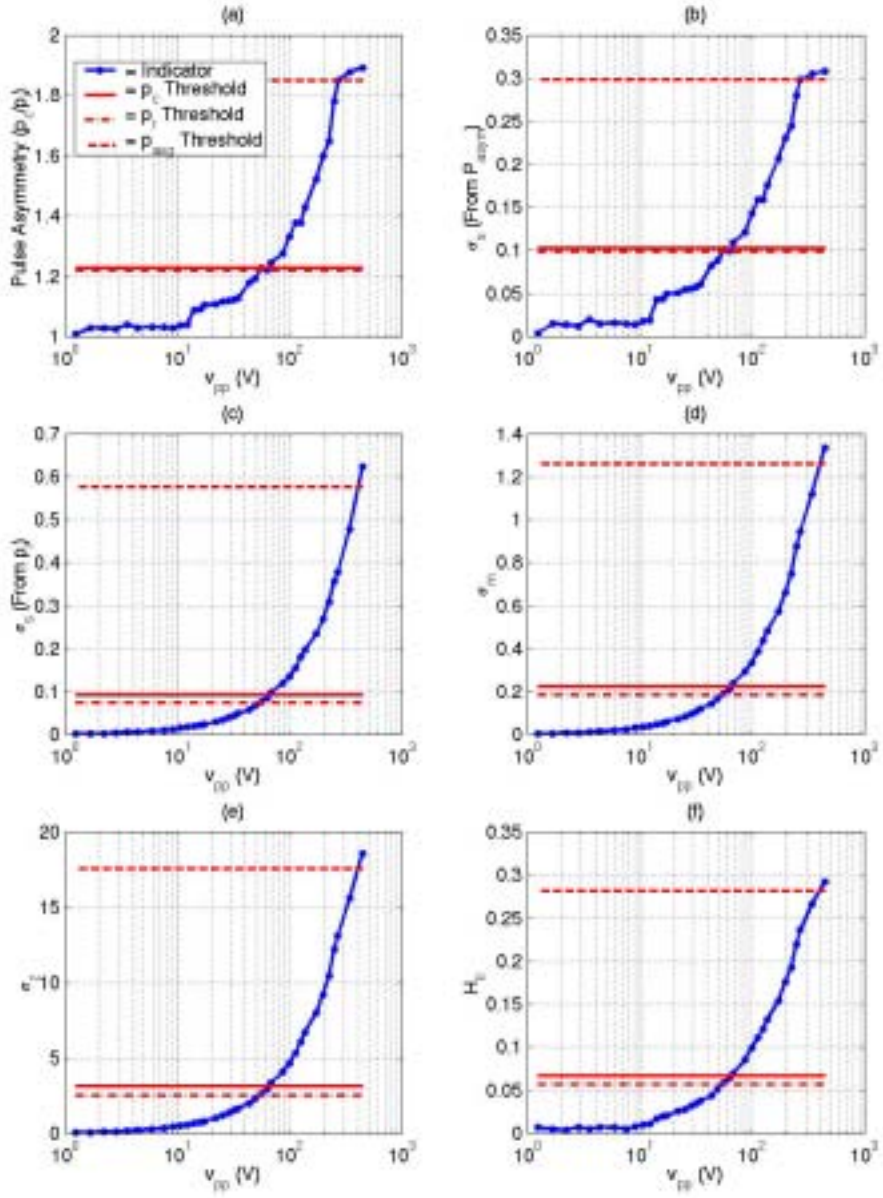

Figure 7.7: First six indicators for a 5.4906 MHz, *f/#* of 1, 1.905 cm diameter transducer excited by a "positive going" "three cycle" pulse. (a) Asymmetric ratio P_{asym}. (b) σ_s from P_{asym}. (c) σ_s from p_r. (d) σ_m. (e) σ_z. (f) Second harmonic ratio H_{II}.

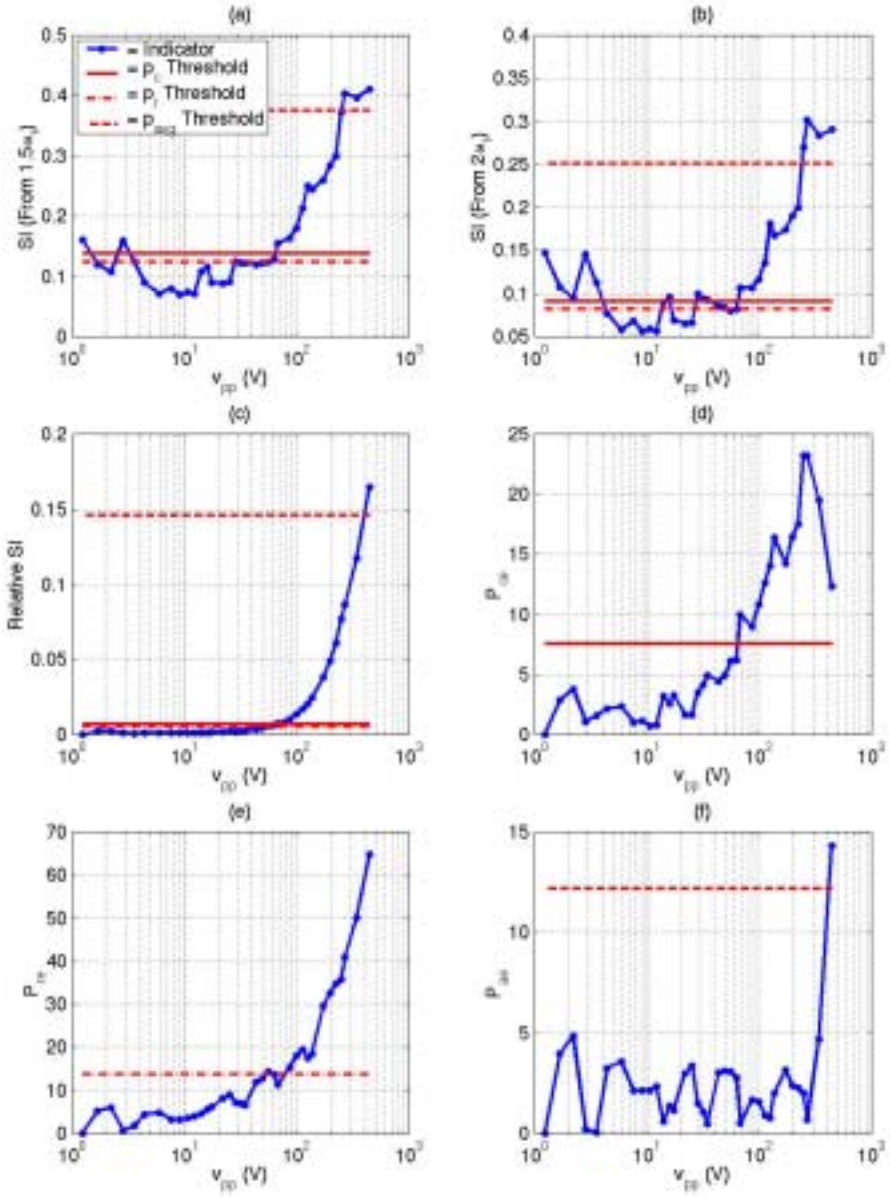

Figure 7.8: Second six indicators for a 5.4906 MHz, *f/#* of 1, 1.905 cm diameter transducer excited by a "positive going" "three cycle" pulse. (a) *si* from $1.5\omega_1$. (b) *si* from $2\omega_1$. (c) *rsi*. (d) P_{ce}. (e) P_{re}. (f) P_{ae}.

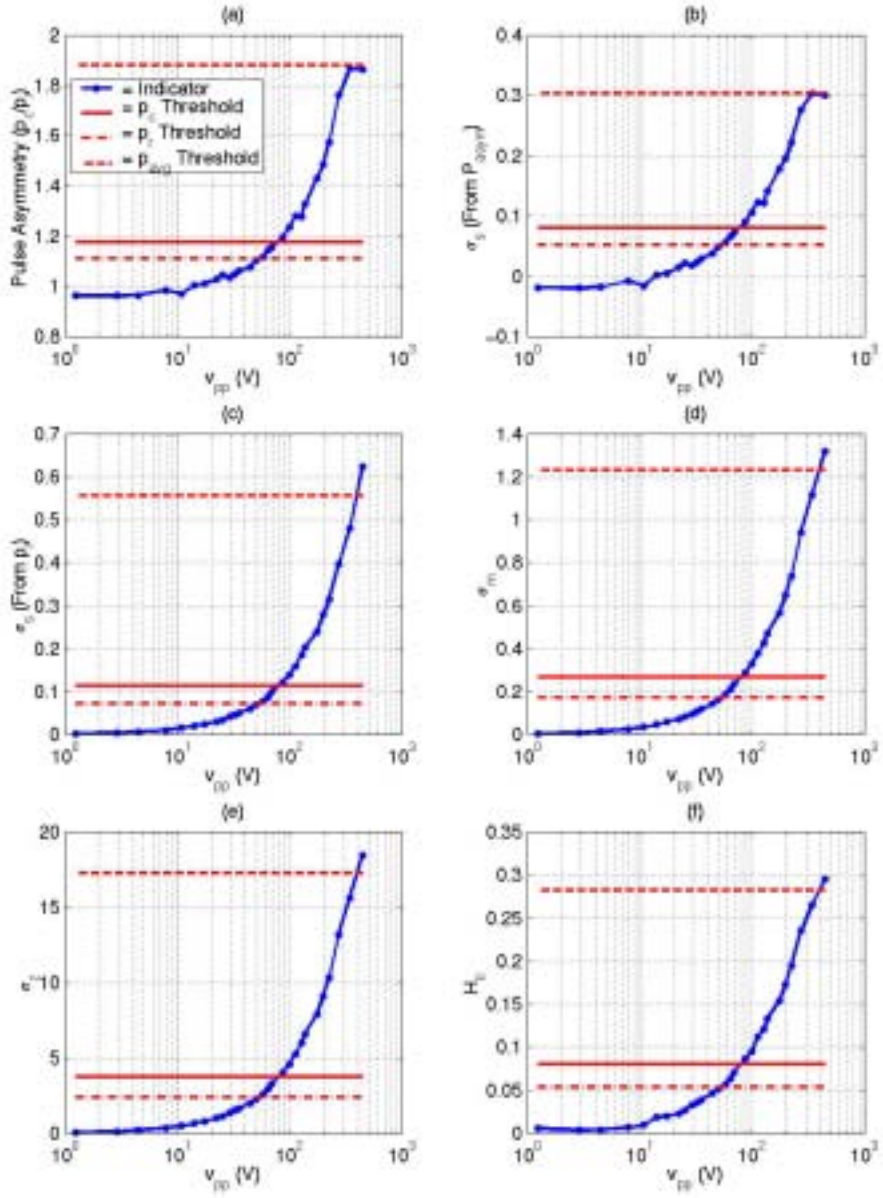

Figure 7.9: First six indicators for a 5.4906 MHz, *f/#* of 1, 1.905 cm diameter transducer excited by a "negative going" "three cycle" pulse. (a) Asymmetric ratio P_{asym}. (b) σ_s from P_{asym}. (c) σ_s from p_r. (d) σ_m. (e) σ_z. (f) Second harmonic ratio H_{II}.

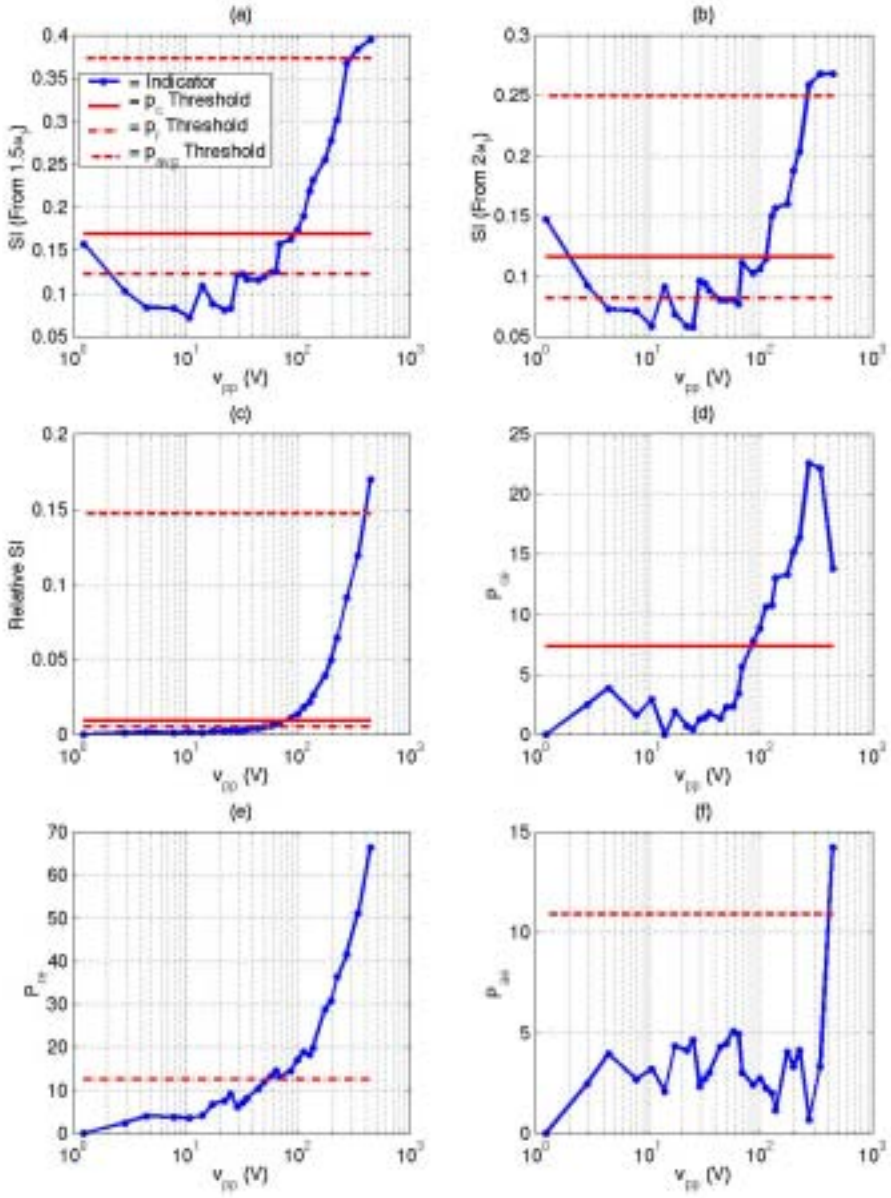

Figure 7.10: Second six indicators for a 5.4906 MHz, *f/#* of 1, 1.905 cm diameter transducer excited by a "negative going" "three cycle" pulse. (a) *si* from $1.5\omega_1$. (b) *si* from $2\omega_1$. (c) *rsi*. (d) P_{ce}. (e) P_{re}. (f) P_{ae}.

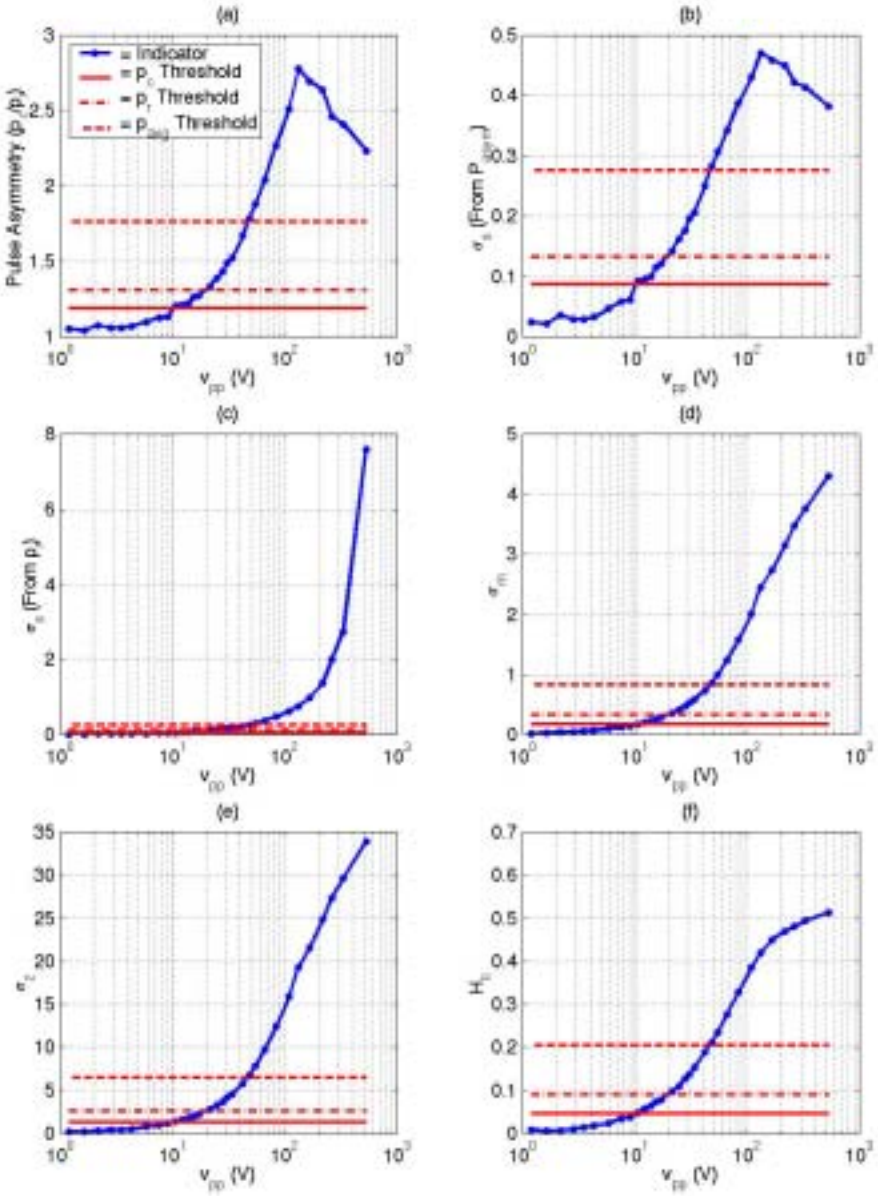

Figure 7.11: First six indicators for a 5.3574 MHz, *f/#* of 2, 1.905 cm diameter transducer excited by a "positive going" "three cycle" pulse. (a) Asymmetric ratio P_{asym}. (b) σ_s from P_{asym}. (c) σ_s from p_r. (d) σ_m. (e) σ_z. (f) Second harmonic ratio H_{II}.

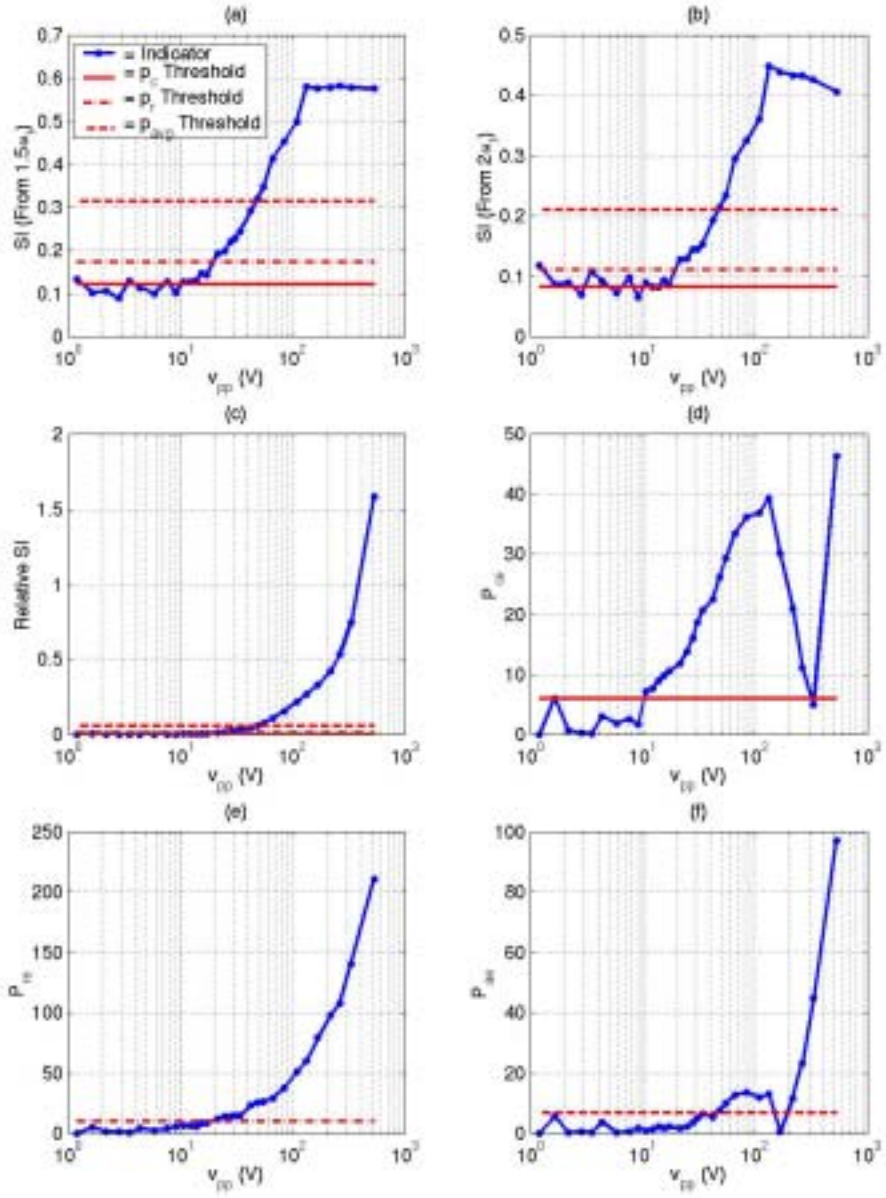

Figure 7.12: Second six indicators for a 5.3574 MHz, *f/#* of 2, 1.905 cm diameter transducer excited by a "positive going" "three cycle" pulse. (a) *si* from $1.5\omega_1$. (b) *si* from $2\omega_1$. (c) *rsi*. (d) P_{ce}. (e) P_{re}. (f) P_{ae}.

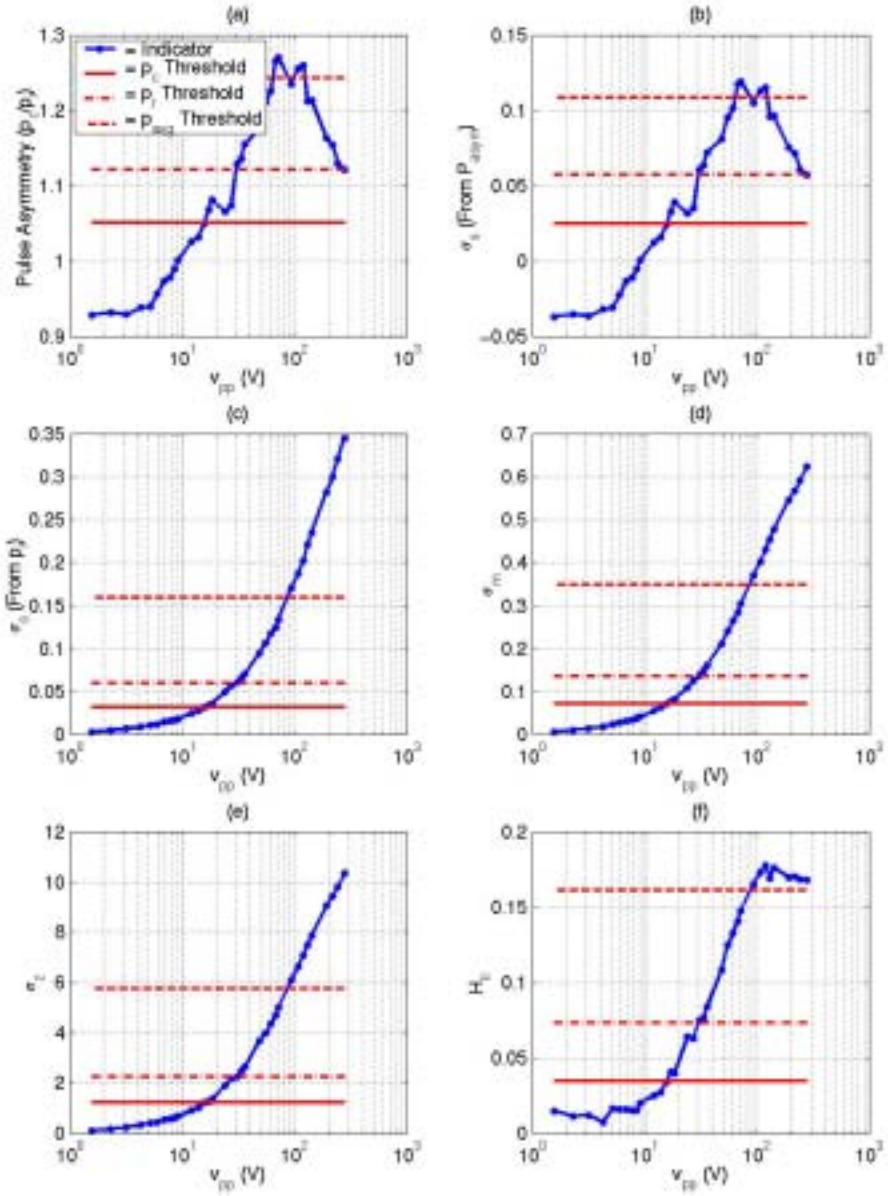

Figure 7.13: First six indicators for a 8.1517 MHz, *f/#* of 1, 1.905 cm diameter transducer excited by a "positive going" "three cycle" pulse. (a) Asymmetric ratio P_{asym}. (b) σ_s from P_{asym}. (c) σ_s from p_r. (d) σ_m. (e) σ_z. (f) Second harmonic ratio H_{II}.

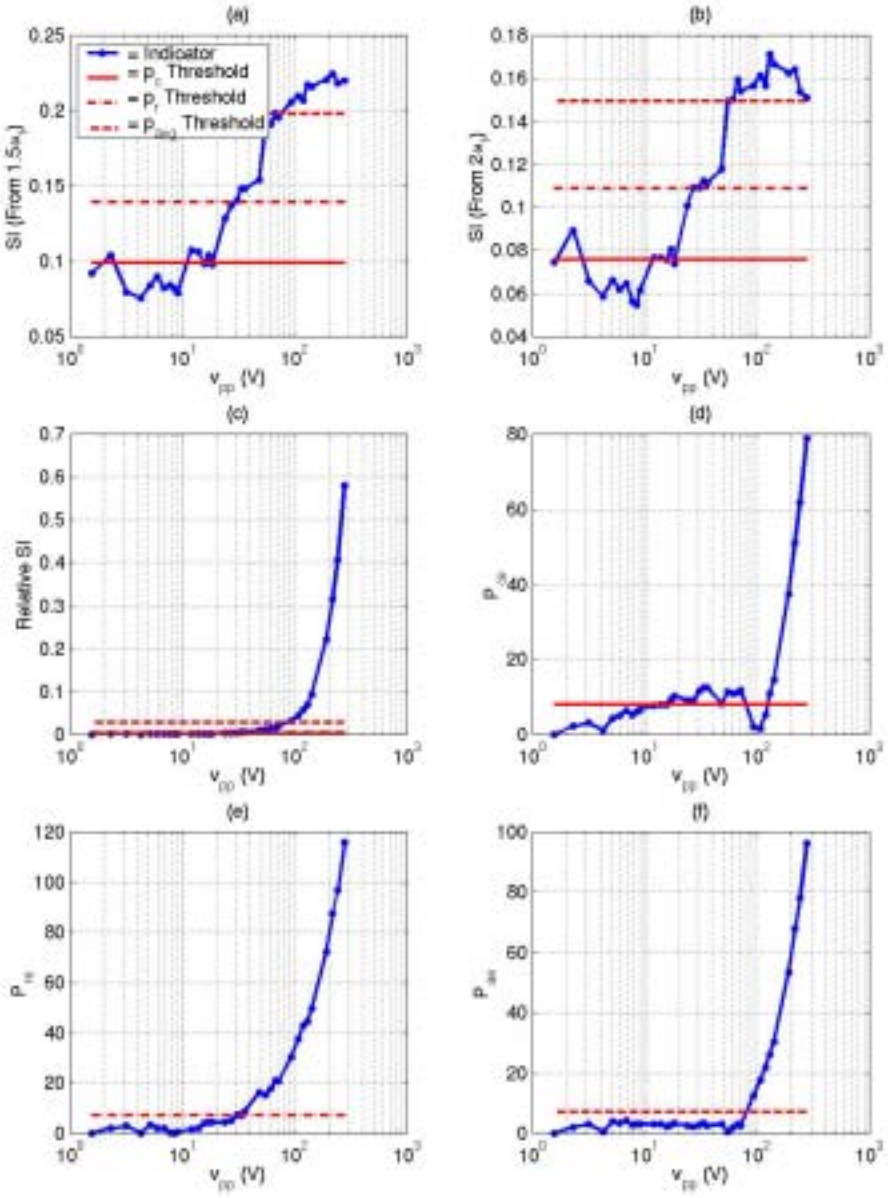

Figure 7.14: Second six indicators for a 8.1517 MHz, *f/#* of 1, 1.905 cm diameter transducer excited by a "positive going" "three cycle" pulse. (a) *si* from $1.5\omega_1$. (b) *si* from $2\omega_1$. (c) *rsi*. (d) P_{ce}. (e) P_{re}. (f) P_{ae}.

The horizontal lines in the figures correspond to the threshold values of the indices as described in the next section. The p_{avg} threshold lines are not plotted on Figures 7.5 and 7.6 because the linear extrapolation error in p_{avg} never exceeded 10%;

hence, a threshold could not be found. Also, the indicator curves in the above plots correspond only to the measured data points without the spline interpolation to be discussed in the Section 7.2.

7.2 Determination of Threshold Values of Indices

Now that the values of the different nonlinear indicators have been found for all of the measurements, the data needs to be processed to determine what the value of the different indices would be when the error in linear extrapolation exceeded some acceptable value. For our experiments, the threshold error level was selected to be 10%. This threshold was chosen because the error in directly measuring the pressure values was often of this same order [*Sempsrott*, 2000]. The goal was then to find the value of the extrapolation factor V_{2sn} from Chapter 5, when the extrapolation error first exceeded the threshold error level. Spline interpolation of the measured values of the indices would then yield the threshold values of the indices at the threshold extrapolation factor.

In order to determine the threshold extrapolation factor, we need to define what is meant by the error in linear extrapolation exceeding the threshold level. The initial approach was to simply find when the P_{ce}, P_{re}, and P_{ae} curves shown in the above plots first intercepted the 10% error line. The value of V_{2sn} at this intersection point would then serve as the threshold extrapolation factor. However, this approach had two problems. First, the location of the intercept varied depending on the choice of the low voltage reference signal. Recall that for my experiments, when determining the relative indicators of nonlinearity, the low voltage reference signal was always selected to be the first measurement in the data set. However, any other measurement in the "linear" range of operation would have also been a valid choice for the reference. Therefore, the variation of this intercept with the choice of the reference signal rendered it incapable of robustly setting the threshold extrapolation factor.

The second problem with using the simple intercept approach to set the location of the threshold extrapolation factor was that it did not reflect how the linear extrapolation would be performed in practice. Namely, in practice, a pressure/voltage measurement would be made for some focal location. Then, if the waveform were sufficiently linear, all LOWER voltage settings would be extrapolated from the measured

data. The simple intercept approach would be equivalent to introducing another low voltage measurement for the sole purpose of extrapolating from this value. In effect, removing the inherent advantage possessed by the absolute indicators of nonlinearity.

Due to these two problems with the simple intercept approach, another method was devised that would be independent of the selection of the reference point and would directly correspond to the real linear extrapolation to be performed. This was done by finding the largest reference value of V_{2sn} for which the error in extrapolating the pressure at all smaller V_{2sn} values would be less than 10%. The first step in the method was to obtain a spline fit to the p_c, p_r, or p_{avg} data points obtained in a particular data set based on the values of V_{2sn} using the "spline" command in MATLAB. The spline fit was chosen over a polynomial fit because it was critical for the curve to pass through the measured data points.

Once the fit was performed, the fit parameters were passed to a function along with the V_{2sn} values and the p_c, p_r, or p_{avg} values. These values would then be used to calculate the P_{ce}, P_{re}, or P_{ae} curves based on some reference V_{2sn} that would also be passed to the function. The P_{ce}, P_{re}, or P_{ae} curve would then be fit by a eighth order polynomial. The polynomial fit was selected so that the value of the error could be extrapolated to a V_{2sn} value of zero. The function then found the peak extrapolation error for all extrapolation voltages between zero and the reference V_{2sn} value, and returned the difference between the peak error and the threshold error of 10%. MATLAB's "fzero" command was then used to determine the reference V_{2sn} value that would cause the function's output to be zero corresponding to the peak error being the same as the threshold error. This particular value for the reference V_{2sn} would then be set as the threshold extrapolation factor.

Clearly, this method for determining the threshold extrapolation factor is independent of the low voltage reference selected for use by the relative nonlinear indicators and also has direct correspondents with how the linear extrapolation would be performed in practice. Furthermore, the method would generate threshold values of V_{2sn} corresponding to p_c, p_r, and p_{avg}. Based on the three threshold extrapolation factors, the three threshold values of the nonlinear indicators can be determined, as will be discussed

shortly. As was shown in Chapter 4, the threshold values for the nonlinear indicators would be different for all three pressure measures of the waveform.

Now that the determination of the threshold extrapolation factors has been discussed, we can develop how these factors would be utilized to determine the threshold values of the nonlinear indicators. These values were found by using MATAB to fit a spline curve to each indicator for each data set based on the V_{2sn} "measured" values. Using this fit, the values of the indicators at the threshold values of V_{2sn} could be interpolated. Once again, a spline fit was selected so that the interpolating curves would pass through the actual data points. The threshold values for each of the nonlinear indicators for each data set are shown as horizontal lines in the figures provided in Section 7.1.

At this point, we are ready to bring in our confidence measure for the experiment. Every experiment needs some measure of believability before any conclusions can be drawn from the results. For our measurements, where the purpose was to evaluate the linearity of a propagating acoustic wave, the main source of error would be nonlinearities in the system prior to the generation of the acoustic wave. However, as was discussed in Chapter 5, these nonlinearities were already quantified in our analysis of the different possible extrapolation factors for every data set considered in the experiment. Furthermore, we can use the error values reported in the ninth column of Tables 5.4, 5.5 and 5.6 to set confidence/error bars for each of the threshold values of the nonlinear indicators.

In order to see how the error bars can be determined, let *dc*, *dr*, and *da* correspond to the error as reported in Table 5.4, 5.5, and 5.6, respectively. Then, repeat the process for finding the threshold values of the nonlinear indicators with the threshold error changed from 10% to 10% ± *dc*/2, 10% ± *dr*/2, and 10% ± *da*/2 for the p_c, p_r, and p_{avg} values, respectively. The error bars for each indicator at each threshold can then be set by

$$Error\_Bar = \left| NI\left(+ d/2\right) - NI\left(- d/2\right) \right| \tag{7.1}$$

where *NI* is the current nonlinear indicator and $\left(\pm d/2\right)$ refers to evaluating the indicator with a threshold error of 10% ± *d*/2 where *d* is either *dc*, *dr*, or *da*. The threshold values for each of the indicators together with their error bars are plotted in Figures 7.15-7.24.

In these graphs, all the results for a particular index for all the data sets have been plotted together for later comparison. Furthermore, the mean value of the index over the data sets is shown as a horizontal line in the plots. Notice that for some of the curves, the uncertainty bars are very small barely being seen about the principle value. These small error bars appear to correspond to the nonlinear indicator flattening out with voltage. Furthermore, the p_{avg} results for the third column have not been plotted because the linear extrapolation error in p_{avg} never exceeded 10% for this data set hence a threshold could not be found.

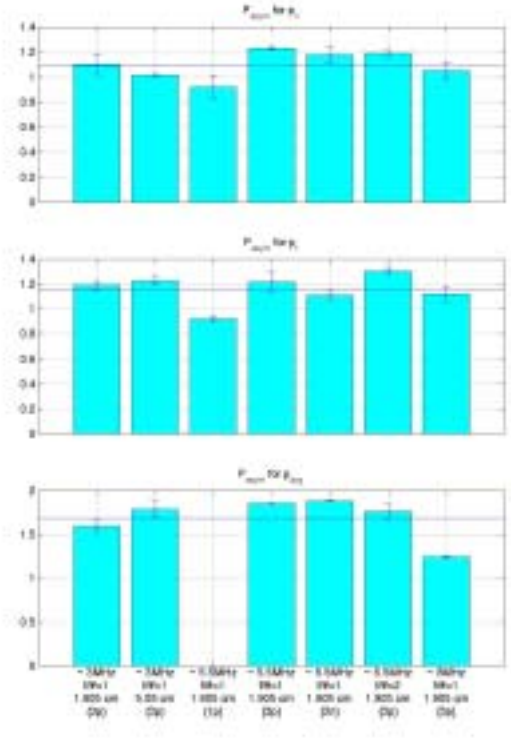

Figure 7.15: Threshold values for the asymmetric ratio.

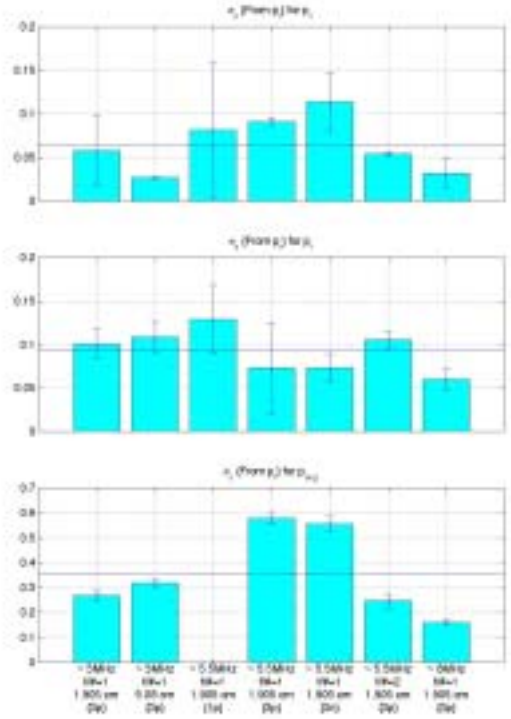

Figure 7.16: Threshold values for σ_s from p_r.

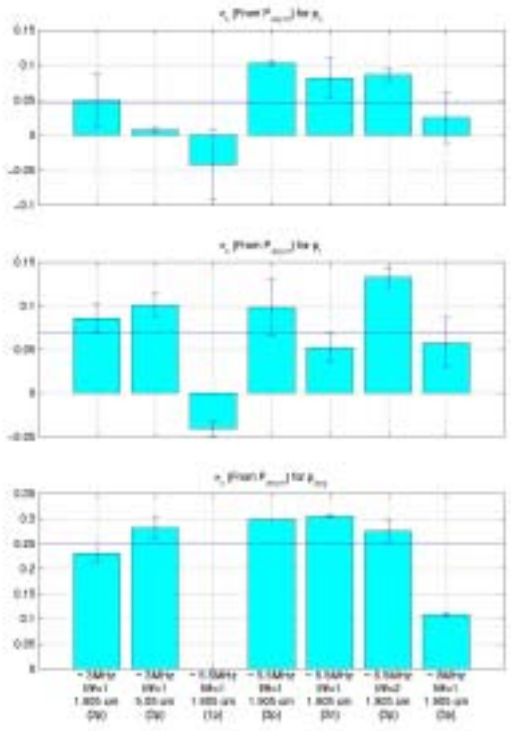

Figure 7.17: Threshold values for σ_s from P_{asym}.

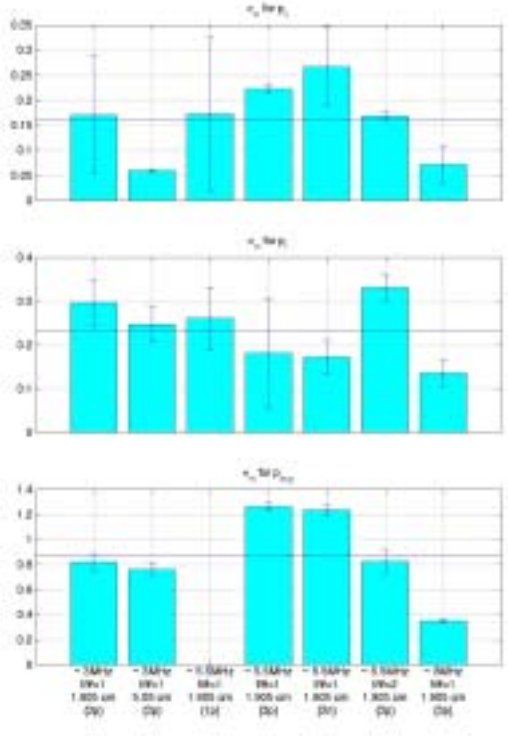

Figure 7.18: Threshold values for σ_m.

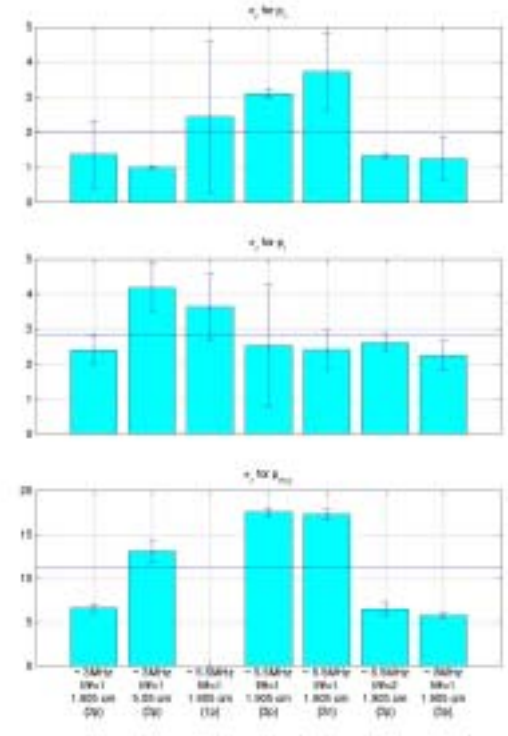

Figure 7.19: Threshold values for σ_z.

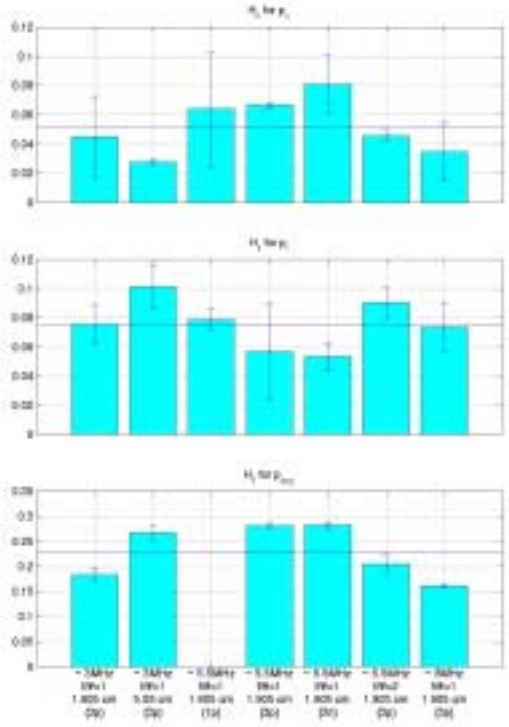

Figure 7.20: Threshold values for the second harmonic ratio.

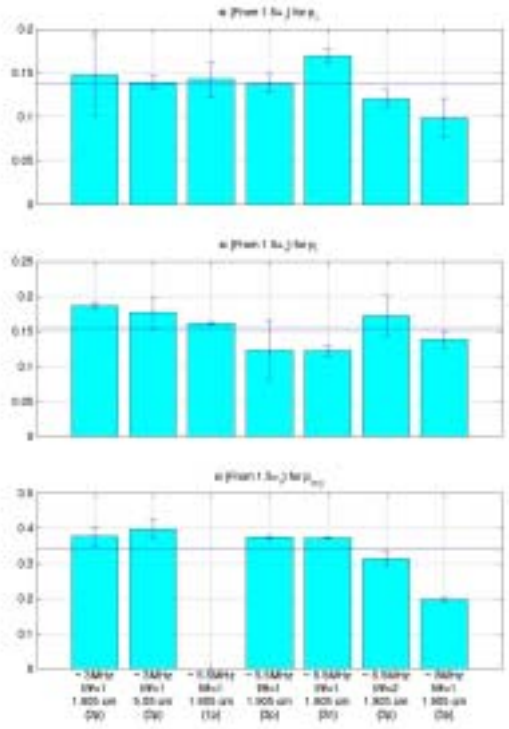

Figure 7.21: Threshold values for *si* from $1.5\omega_1$.

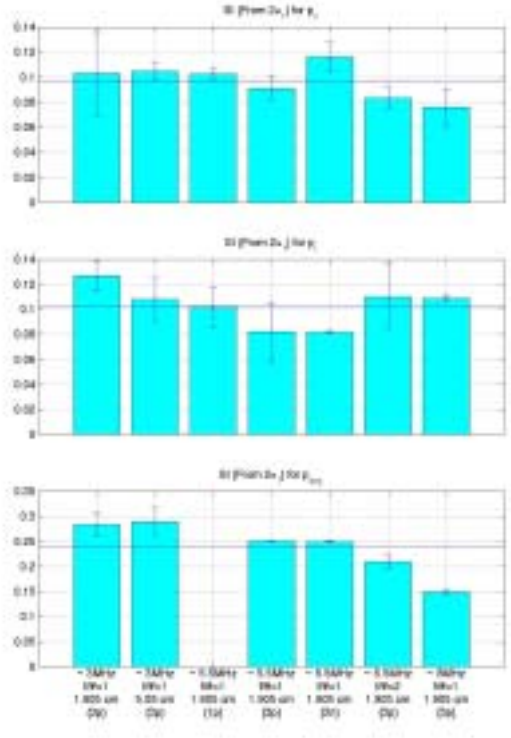

Figure 7.22: Threshold values for *si* from $2\omega_1$.

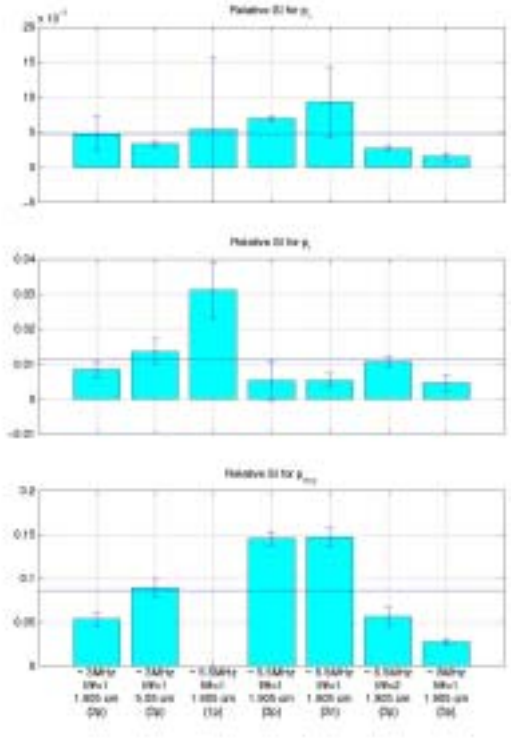

Figure 7.23: Threshold values for *rsi*.

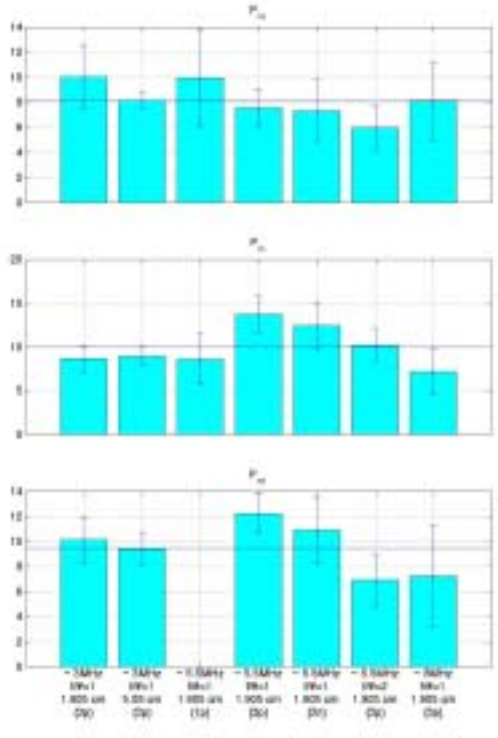

Figure 7.24: Threshold values for the relative focal pressure.

7.3 Evaluation of the Different Indices

Now that the threshold values for the different indices have been determined, we can evaluate the proposed indices as possible candidates to govern voltage-based linear extrapolation. To this end, we need to define what properties a successful indicator would possess. First, a successful indicator would need to be robust to transducers operating at different frequencies, with different bandwidths, and different phase as well as to transducers with different *f/#*'s and aperture dimensions. Therefore, the successful indicator would yield the same threshold values for all the data sets considered in the experiment. Of course, by "the same" we mean to within the confidence bars set in Section 7.2.

As well as being consistent between data sets, the successful indicator would also be well behaved within each data set. This means that the indicator can only achieve the threshold value at the threshold error setting. Otherwise, it would be impossible from a single measurement to determine where the current value of the nonlinear indicator

should be positioned on the nonlinear indicator curve. For the indicators considered in this thesis, this means that the ideal indicator would be strictly monotonically increasing.

At this point, we are ready to evaluate each of the proposed indices. Since consistency between data sets was deemed the most important evaluation criterion, the indices will first be evaluated on this basis. Upon examining the plots shown in Figures 7.15 through 7.24, it is clear that none of the indicators are completely consistent. In all cases, the mean value "misses" at least one of the error bars for one of the data sets. This is particularly evident for extrapolation of the p_{avg} values that clearly have the largest variation in their threshold values. A possible explanation for the lack of consistency can be found by comparing the behavior of the focal pressures for a couple of the data sets. The plots in Figure 7.25 are the measured pressure values from the focus for the (a) ~5.5 MHz f/#1 transducer, the (b) ~5.5 MHz f/#2 transducer, and the (c) ~8 MHz f/#1 transducer evaluated in this study. The diameter of all three transducers is 1.905 cm, and each is excited by a "three cycle" "positive going" waveform.

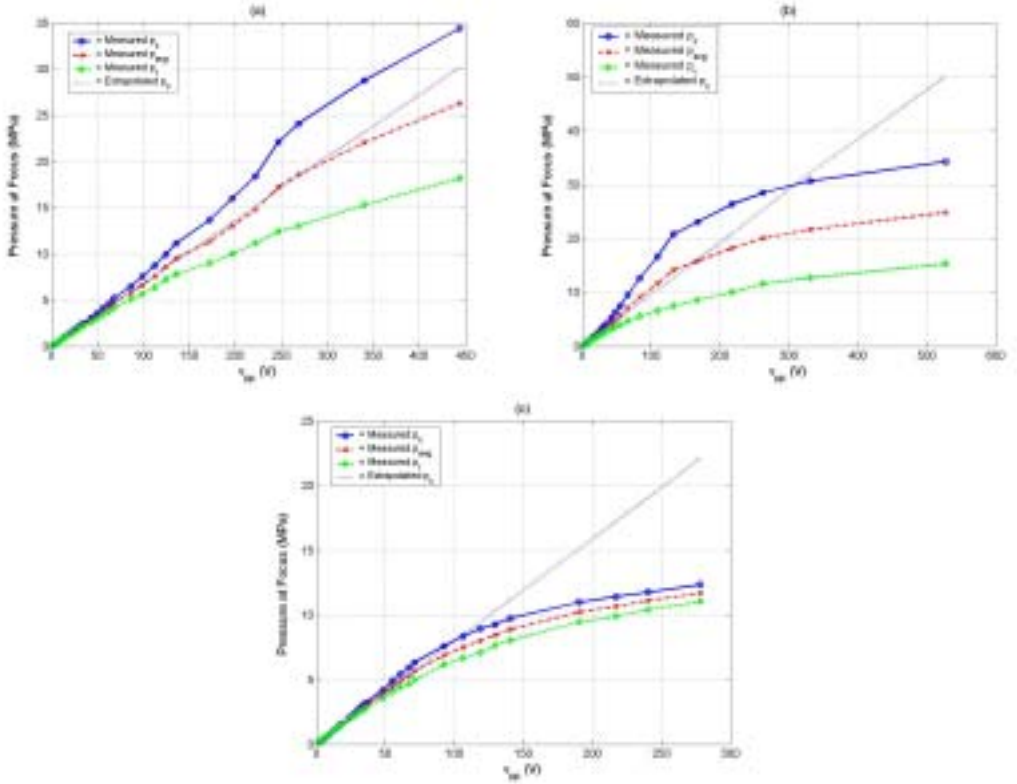

Figure 7.25: Direct comparison of pressures at the focus. (a) ~5.5 MHz *f*/#1 transducer (b) ~5.5 MHz *f*/#2 transducer (c) ~8 MHz *f*/#1 transducer.

Notice that in all three plots, p_c initially increases away from the linearly extrapolated line due to asymmetric distortion. However, as nonlinear absorption increases and the transducer approaches saturation, the p_c values approaches the extrapolation line once again and even crosses the line for plots (b) and (c). Although this general trend is observed in all three plots, the separation between the onset of nonlinearity where the p_c value first moves above the line and the recrossing of the extrapolation line does not remain the same. The relative importance of nonlinear absorption to asymmetric distortion seems to increase as the *f/#* and frequency increase with a stronger dependence on the frequency.

The above analysis can also be extended to the p_{avg} values. Notice that in plot (b) of Figure 7.25, the p_{avg} value also increases away from the extrapolation only to later cross at a higher voltage value. Many of the data sets analyzed exhibited this same type of behavior in the p_{avg} values so plot (b) is not an unusual exception. However, for plots (a) and (c), the p_{avg} value never increases above the extrapolation line but simply drops below the line as the voltage increases. This effect would probably also be present for p_c for some transducers since this is just a natural extension of the trend in the separation between the onset of nonlinearity and the recrossing of the extrapolation line that was discussed in the previous paragraph. However, in the p_{avg} case there is no longer a connection between the separation and the *f/#* or frequency. Recall that the p_{avg} values depend on both the p_c values and the p_r values. Therefore, the lack of a connection implies that the relative importance of nonlinear absorption and asymmetric distortion for the p_r values must also be affected by the *f/#* and frequency in a similar manner to how they were affected for the p_c values.

An important conclusion can be drawn from our observations on the relative effects of nonlinear absorption and asymmetric distortion. Recall that when the different indicators were introduced in Chapter 4, not one of the indicators attempted to capture the effects of both nonlinear absorption and asymmetric distortion. Ostrovskii/Sutin's σ_s focused on asymmetric distortion with the neglecting of nonlinear absorption, and Bacon's σ_m neglected distortion and focused on saturation or nonlinear absorption effects. The frequency domain indices, such as *si*, could potentially capture both effects but are not based on a quantitative theory, so there is no guarantee. Hence, the change in

the relative importance of the two nonlinear effects of asymmetric distortion and nonlinear absorption is what generates the inconsistency in the nonlinear indicators. Therefore, although none of the current indicators are consistent, it may be possible to find a consistent indicator by further developing the theory to include both effects.

Since the development of any theory would rely heavily on simplifying assumptions, we can also use our results on the threshold values for the different indices to help guide these future assumptions. Notice that the threshold values of σ_m are very different from the value of 2 predicted by Bacon's theory for p_{avg}, whereas the threshold values of σ_s often approach the predicted values of 0.1 and 0.316 for $p_{c,r}$ and p_{avg}, respectively. Therefore, any future developments of the theory should probably be based on the foundation already laid by Ostrovskii and Sutin discussed in Chapter 2.

Before concluding our evaluation of the proposed indices, it is important to elaborate on the consistency issue for the relative focal pressures. The results shown in Figure 7.24 were obtained using the threshold extrapolation factor as the reference for the linear extrapolation. However, the low voltage measurement could also be used for the extrapolation. This would enforce consistency across all of the data sets by forcing the threshold value for the relative focal pressure to be 10%. Although, this method would yield a consistent indicator, the relative focal pressure would still not serve as a good indicator for nonlinearity when extrapolating the p_c or p_{avg} values due to a lack of monotonicity. However, P_{re} could be used as a reliable indicator for p_r extrapolation.